ChemComm

Accepted Manuscript

This article can be cited before page numbers have been issued, to do this please use: M. K. Bayazit, S. Moniz and K. Coleman, *Chem. Commun.*, 2017, DOI: 10.1039/C7CC04044J.

ROYAL SOCIETY OF CHEMISTRY

rsc.li/chemcomm

View Article Online
DOI: 10.1039/C7CC04044J

Journal Name

COMMUNICATION

Gram-scale production of nitrogen doped graphene using a 1,3-dipolar organic precursor and their utilisation as stable, metal free oxygen evolution reaction catalysts

Received 00th January 20xx,
Accepted 00th January 20xx

DOI: 10.1039/x0xx00000x

www.rsc.org/

Mustafa K Bayazit,[a,b *] Savio J. A. Moniz[b*] and Karl S. Coleman[c]

For the first time, a one-step scalable synthesis of a few-layer ~10% nitrogen doped (N-doped) graphene nanosheets (GNSs) from a stable but highly reactive 1,3-dipolar organic precursor is reported. The utilization of these N-doped GNSs as metal-free electrocatalysts for the oxygen evolution reaction (OER) is also demonstrated. This process may open the path for scalable production of other heteroatom doped GNSs by using the broad library of well-known, stable 1,3-dipolar organic compounds.

Fabrication of nitrogen doped (*N*-doped) carbon nanomaterials has received significant interest due to their potential application in supports for catalysts, membrane technology, sensors and supercapacitors.[1] Among the *N*-doped carbon nanomaterials, particular consideration has been given to *N*-doped graphene nanosheets (*N*-doped GNSs). For instance, the *N*-doped GNSs with pyridinic, pyrrolic and/or graphitic N moieties have been demonstrated to display higher catalytic activity for the oxygen reduction reaction (ORR) compared to commercial Pt/C catalysts in applications such as metal–air batteries and fuel cells.[2] It was also shown that *N*-doped GNSs are extremely versatile and exhibit high reversible capacity, superior rate capability as well as long-term cycling stability.[1j] However, there are very few reports of their utilization as metal-free electrocatalysts for the oxygen evolution reaction (OER).[3] To date, several synthetic strategies including chemical vapor deposition, arc discharge, and thermal/plasma treatment have been developed to prepare *N*-doped GNSs with varying elemental nitrogen compositions and environments.[4] These approaches usually require special reaction conditions (*e.g.* plasma, inert atmosphere, high pressure *etc.*), only proceed at high temperatures (800-1000 °C), and use toxic precursors (*e.g.* chlorinated hydrocarbons, cyanuric chloride *etc.*).[4a] However an environmentally benign precursor, chitosan, has also been demonstrated to yield high-quality single layer N-doped graphene films, although relatively high temperatures between 600-800 °C were employed.[5] In order to scale-up the preparation of *N*-doped GNSs for practical applications, novel, cost effective and less labour-intensive strategies are required. Considering the broad library of well-known 1,3-dipolar organic compounds containing various heteroatoms (*e.g.* nitrogen, sulphur and phosphorous) or their mixtures, 1,3-dipolar cycloaddition polymerization reactions could be utilized as a scalable, low-cost method to synthesize heteroatom containing carbon-based nanostructures. However, to the best of our knowledge no cycloaddition reaction-based synthetic protocol has been reported for the preparation of heteroatom doped graphene or related structures,[4a, 6] although solution-mediated Diels-Alder polymerization,[7] cyclodehydrogenation of bianthryl-based linear polymers[8] and the [2+2] cycloaddition of octafunctionalized biphenylenes[9] were shown to be successful for the preparation of graphene-like nanostructures.

In our previous work we reported that the self-cycloaddition of an *in-situ* prepared pyridinium ylide dipole can yield conjugated fluorescent indolizine structures through the addition of a second ylide to the double-bond of pyridine heterocycle.[10] This was shown to occur at a temperature of 150 °C during the surface modification of single-walled carbon nanotubes (SWCNTs). Free indolizine formation in the absence of an additional reactant revealed that the double bonds in the aromatic ring could act as reactive dipolarophiles under suitable reaction conditions. This phenomenon can be extended in order to synthesize conjugated heterocyclic systems and high molecular weight polymers under suitable reaction conditions, for example, the [2+2] cycloaddition polymerisation of alkenes.[11] In this respect, phthalazinium-1-olates can be used as versatile precursors due to their high reactivity and stability in air.[12] For example, 3-phenyl-phthalazinium-1-olate can be readily prepared under ambient conditions with high yields using phthalic anhydride and phenyl hydrazine derivatives, and can be stored for long periods without decomposition.[13] Reactivity and stability of phthalazinium-1-olates towards conjugated double-bonds was previously demonstrated under solvent-free conditions (220 °C) to introduce nitrogen rich phenylphthalazine groups on the SWCNT surface via a 1,3-dipolar cycloaddition pathway.[14]

[a] *Department of Chemistry, Imperial College London, London SW7 2AZ, UK.*
[b] *Department of Chemical Engineering, University College London, Torrington Place, London, WC1E 7JE, UK.*
[c] *Department of Chemistry, Durham University, South Road, Durham DH1 3LE, UK.*
E-mail: m.bayazit@imperial.ac.uk, s.moniz@ucl.ac.uk

Electronic Supplementary Information (ESI) available: TEM, AFM of *N*-doped GNSs, TGA of *N*-doped GNSs, C 1s and O 1s XPS and FTIR spectra of *N*-doped GNSs and electrochemical stability of *N*-doped GNSs. See DOI: 10.1039/x0xx00000x

View Article Online
DOI: 10.1039/C7CC04044J

Journal Name

COMMUNICATION

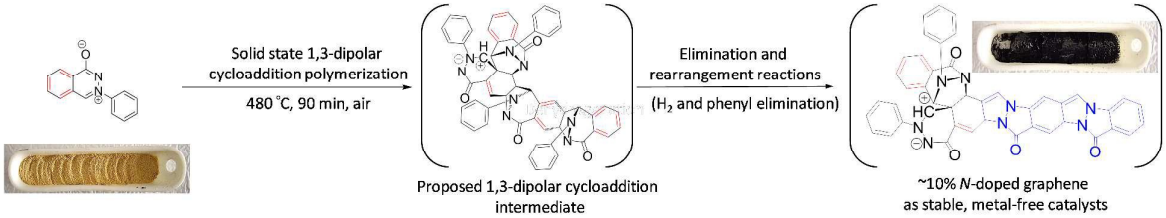

Scheme 1. Formation of *N*-doped graphene nanosheets via a 1,3-dipolar self-cycloaddition of 3-phenyl-phthalazinium-1-olate. Possible 1,3-dipole/dipolarophile interactions are anticipated to take place on the electron deficient fused benzene ring, in which the double bonds are highlighted in red on both the 3-phenyl-phthalazinium-1-olate and likely intermediate structure. Note that the decomposition of both precursor and oligomeric carbonized products are also expected at 480 °C in air. The blue region shows the possible planar structure. The orange and black materials in the ceramic boats are 3-phenyl-phthalazinium-1-olate and the resultant *N*-doped graphene, respectively.

Herein, we report the first example of the utilization of 1,3-dipolar cycloaddition reactions to fabricate gram-scale *N*-doped GNSs using a nitrogen rich 1,3-dipole, namely 3-phenyl-phthalazinium-1-olate, as the only precursor via a mild thermal treatment in air. The *N*-doped GNSs were used as a stable, metal-free catalyst for electrocatalytic oxygen evolution reaction (OER). In a typical procedure, 3-phenyl-phthalazinium-1-olate containing approximately 12% nitrogen (*at%*) is carbonized at 480 °C in air to yield *N*-doped GNSs (**Scheme 1**). Similar to the previous studies,[10-11] *N*-doped GNSs are believed to be formed following the successive 1,3-dipolar cycloaddition of 3-phenyl-phthalazinium-1-olate to the reactive double-bonds present on an electron deficient fused benzene ring at relatively high temperatures, as shown in **Scheme 1**. Raman spectroscopy has been used extensively to study graphitic materials, with the *D-band* at *ca.* 1350 cm^{-1} linked to the sp^3*-type* surface defects and can be easily compared to the tangential band (*G-band*) at *ca.* 1580 cm^{-1}.[15] The Raman spectra (632.8 nm excitation, 1.96 eV) of the produced carbonaceous material is shown in **Figure 1a**, which confirms the formation of a graphitic material. The *N*-doped GNSs showed an I_D/I_G ratio of 0.68, attributed to disruption of the graphitic framework in comparison to a non-defective graphite surface.[15]However this ratio was smaller than the previously synthesized *N*-doped graphene structures which exhibited a I_D/I_G ratio in the range of 0.86 to 0.98 for different *N*-doping levels (10.1-5.6 N%).[16] These findings suggest that the *N*-doped GNSs produced via the 1,3-dipolar self-cycloaddition polymerisation route contain less sp^3*-type* defects. In fact, surface functionalization of *N*-doped GNSs, which lead to an increase in the I_D/I_G ratio, are mainly expected as a result of our synthetic method since the reaction proceeds via a 1-3-dipolar cycloaddition to the double-bonds on the surface. Less sp^3 defects are sought-after as highly defective *N*-doped GNSs suffer from reduced electron transport on the surface which can limit their catalytic performance.[4a] Thus less defective *N*-doped GNSs produced by our 1,3-dipolar self-cycloaddition polymerisation route may be beneficial for catalytic reactions such as ORR/OER since electron mobility will be improved. In addition, the characteristic *2D-band* is observed around 2640 cm^{-1} which is in close agreement with the previously reported few-layer GNSs.[15] The structure of the as-produced *N*-doped GNSs was further studied by X-ray diffraction, which exhibited a broad [002] reflection at 21.46° 2θ, corresponding to a *d*-spacing of 0.41 nm (**Figure 1b**). This increased interlayer spacing, compared to pure graphite (0.37 nm), can be attributed to the introduction of surface groups such as nitrogen containing 5-membered heterocycles into the 2D carbon framework. The other peak at *ca.* 44.65° 2θ corresponds to the [100] in-plane hexagonal atomic arrangement. Transmission electron microscopy (TEM) images show the presence of a 2D, layered carbon nanomaterial (**Figure 1c**). The presence of partially transparent sheets suggests that *N*-doped GNSs can be exfoliated in amidic organic solvents (e.g. NMP and DMF) which has been shown to be effective for carbon nanomaterial exfoliation.[17] The TEM image of the *N*-doped GNSs exhibits some characteristics associated with the formation of slightly twisted GNSs, which might be related to the regioselectivity of the cycloaddition polymerisation process, possibly occurring perpendicular to the plane of the 1,3-dipole

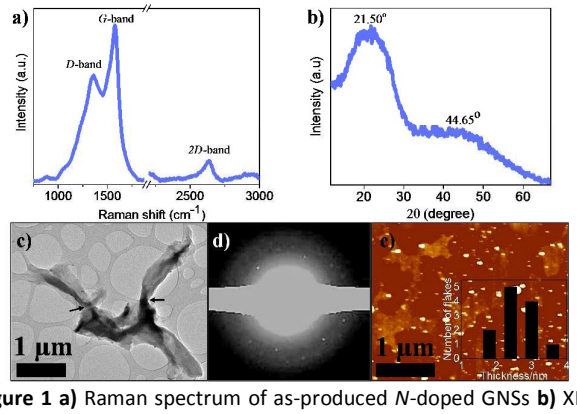

Figure 1 a) Raman spectrum of as-produced *N*-doped GNSs **b)** XRD pattern of as-produced *N*-doped GNSs **c)** TEM image *N*-doped GNS dispersed in NMP. Black arrows show the twisted regions. **d)** The selected area electron diffraction (SAED). **e)** AFM image with the inset showing average thickness of *N*-doped GNS dispersed in NMP.

View Article Online
DOI: 10.1039/C7CC04044J

(see **Scheme 1**). Further TEM analysis suggests the formation of 3D-network like layered structures (see ***ESI Figure S1***). Upon further inspection, the selected area electron diffraction (SAED) displays a ring-shaped pattern with several diffraction spots, due to the stacking of crystalline graphitic layers with different angles (**Figure 1d**).[18] AFM height image and the thickness distribution reveal the emergence of *N*-doped GNSs with lateral dimensions of ~0.5-3 µm and approximately 2.5±0.5 nm in thickness (**Figure 1e** and **inset** and ***ESI Figure S2***). The FT-IR spectrum of the *N*-doped GNSs shows a sharp peak at 1595 cm^{-1} which is attributed to the C-C stretching bands present in the graphene framework (see ***ESI Figure S3***). There were no obvious C=O stretchings present in the 1650 to 1800 cm^{-1} range except a small shoulder at 1657 cm^{-1} which is due to the formation of a 6-membered lactam ring following cycloaddition polymerization. Thus the enhanced *D-band* in the Raman spectrum of *N*-doped GNSs may also be correlated to edge effects rather than purely chemical defects.[19] X-ray photoelectron spectroscopy (XPS) was employed to study the elemental composition of the obtained *N*-doped GNSs. As expected, the XPS survey spectrum of *N*-doped GNSs shows the presence of C, O and N atoms in 73.18, 17.18 and 9.64 atomic per cent (at %) ratios respectively (**Figure 2a**). The percent of atomic nitrogen in the *N*-doped GNSs (9.64%) was comparable to that of the 1,3-dipole precursor (11.74%), which indicates almost complete retention of nitrogen atoms after polymerisation. This correlation provides additional evidence that the *N*-doped GNSs are formed via a 1,3-dipolar self-cycloaddition polymerization, rather than a thermal decomposition of the dipole structure at high temperatures. However, it is worth noting that the percentage of oxygen in *N*-doped GNSs was higher than the 1,3-dipole precursor, suggestive of surface oxidation (e.g. oxides) in air. Figure 2b shows the deconvoluted N 1s XPS spectra of *N*-doped GNSs which was fitted by two peaks; they can be attributed to pyrrolic nitrogen (*ca.* 400.2 eV) and pyridinic nitrogen (398.7 eV) with 62.3 % and 37.7 % contributions, respectively.[4a, 20] Obtaining pyrrolic nitrogen-rich *N*-doped GNSs is not surprising since the 1,3-dipolar cycloaddition of 3-phenyl-phthalazinium-1-olate mainly yields 5-membered pyrazole-type ring structures which confirms the previously proposed reaction pathway. Furthermore, the deconvoluted C 1s XPS spectrum of the *N*-doped GNSs exhibits three peaks at *ca.* 284.7, 285.9 and 288.9 eV, ascribed to sp^2 carbon with C=C bonds (70.57 %), C=N (20.81 %) and the physisorbed oxygen (8.62 %) respectively, consistent with previous reports (see ***ESI Figure S4***).[16, 21] The thermal stability of the synthesised *N*-doped GNSs was studied by thermogravimetric analysis (TGA) in both air and helium (see ***ESI Figure S5***). The TGA curve indicates that the *N*-doped GNSs decompose at *ca.* 545 °C, similar to graphene (500-600 °C),[22] indicative of good thermal stability.[23] Consistent with the evolution of nitrogen functionalities in carbonaceous materials during pyrolysis,[24] *N*-doped GNSs exhibited only 25% weight loss at *ca.* 900 °C in air, which may be linked to the formation of stable quaternary nitrogen moieties during TGA that restricts *N*-oxide formation and subsequent decomposition of the material. Furthermore, similar weight loss, attributed to covalently-attached surface groups and physisorbed oxygen, was observed at *ca.* 900 °C in helium as well (see ***ESI Figure S5***). The greater rate of weight loss in helium suggests the formation of quaternary nitrogen moieties is slower than that in air.

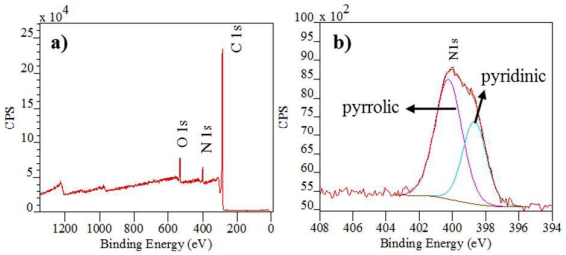

Figure 2 a) XPS survey spectrum and **b)** N 1s XPS spectrum of as-produced *N*-doped GNSs.

To evaluate the electrocatalytic activities of *N*-doped GNSs, we chose to investigate their activity towards the oxygen evolution reaction (OER), which has recently been the focus of much attention.[3b] We deposited *N*-doped GNSs onto both inert carbon paper and Nickel foam substrates via a simple drop-casting method using Nafion as a binder (see Experimental section for further details) and tested them in 1M KOH solution (pH 14). RuO_2 on Nickel foam was used as a comparison. Compared to the uncoated carbon paper, the onset for OER in the *N*-doped GNS was found at approximately 1.5 V vs RHE and achieved a current density of *ca.* 55 mA/cm^2 at 1.8 V. Similarly, *N*-doped GNS coated on Nickel foam showed an onset of 1.4 V vs RHE and achieved a current of *ca.* 100 mA/cm^2 at 1.8 V (**Figure 3**). Upon the application of potentials above the onset potential, the evolution of bubbles (oxygen) on the *N*-doped GNS electrode and hydrogen bubbles on the Pt counter electrode was evident. The small redox peak at *ca.* 1.4 V in *N*-doped GNS is likely due to some impurity nickel oxide species on the Nickel foam substrate; the C-V trace from the *N*-doped GNS electrode is highly reproducible after scanning several times. The OER activity is higher than that obtained for *N*-doped graphene/SWCNT hybrids (*ca.* 7.5 mA/cm^2 at 1.6V vs RHE)[25] but onset and total current a little lower than a benchmark, such as RuO_2. Furthermore, the activity is of the order of that obtained for *N*-doped graphene nanoribbon networks (ca. 15 mA/cm^2 at 1.6 V vs RHE) recently reported, which is not surprising as both of these *N*-doped graphenes possess electron-withdrawing pyridinic N moieties, which can accept electrons (p-type doping) from adjacent C atoms (δ+), facilitating the adsorption of water oxidation intermediates (OH^-, OOH^-).[3] This is effectively the rate-determining step for OER in alkaline solution and thus provides reasoning for OER activity in *N*-doped graphenes in contrast to non-doped carbons that only exhibit high conductivity and no appreciable catalytic activity. From DFT studies, the OER active sites have been identified in *N*-doped graphene nanoribbons at the carbon atoms near the nitrogen atom which possess a minimum theoretical OER overpotential of 0.405 V, which is comparable to Pt-containing catalysts.[26] Electrochemical stability of the N-doped GNS electrodes on both carbon paper and nickel foam substrates was also tested under a fixed overpotential (1.7 V vs RHE) over 24-hours of continued water electrolysis (see ***ESI Figure S6***). The metal-free N-doped GNS catalyst showed excellent stability with no obvious loss of current under rapid stirring, which was employed in order to force the removal of the accumulated oxygen bubbles from the N-doped GNS surface during water electrolysis. In contrast, the RuO2 displayed inferior stability in KOH, losing over 50% of the activity within the first 10 minutes (see ***ESI Figure S7***) and is a common observation for Ru-based electrocatalysts in

View Article Online
DOI: 10.1039/C7CC04044J

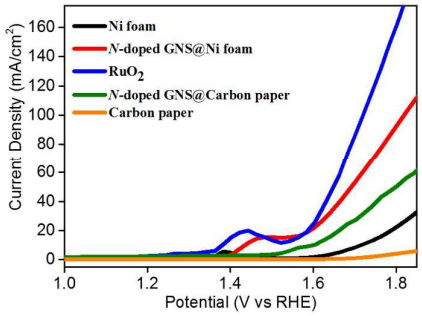

Figure 3 Current-voltage curves of *N*-doped GNS dispersed in DMF and deposited on both carbon paper and Nickel foam together with pure carbon paper and Nickel foam and RuO_2 on Nickel foam for the oxygen evolution reaction (OER), carried out in 1M KOH (pH 14).

Redox peak for RuO_2 is due to the Ru^V/Ru^{IV} redox couple.[27] alkaline conditions.[27] Thus the N-doped GNS could be utilised as a low-cost, metal free stable electrocatalyst for OER and potentially as a co-catalyst for photocatalytic water oxidation, work of which iscurrently underway.

In summary, for the first time, a 1,3-dipolar cycloaddition reaction was tested and proven to be a suitable synthetic technique for gram-scale production of few-layer 10% *N*-doped GNSs containing less sp^3*-type* defects, which was isolated as a stable solid under relatively mild conditions. Photoelectron spectroscopy revealed that *N*-doped GNSs only possessed pyridinic and pyrrolic nitrogen moieties, the result of a 1,3-dipolar self-cycloaddition polymerisation process which can only produce 6- and 5-membered rings under the aforementioned experimental conditions. The *N*-doped GNSs exhibited good thermal stability up to 545 °C and yielded approximately 75% carbonized material at 900 °C in air, and could potentially be used in heat resistant coatings and similar applications. Moreover, the utilisation of *N*-doped GNSs as efficient and stable electrocatalysts for OER has been demonstrated, which opens the path toward their utilisation as metal-free electrocatalysts for the kinetically and thermodynamically challenging process of water oxidation, brought about by the presence of electron-withdrawing pyridinic nitrogen groups. We further anticipate that this scalable high yielding fabrication process for *N*-doped GNSs will pave the way for the development of other applications that require large amounts of *N*-doped carbons in order to be low-cost and sustainable. In addition, other heteroatom doped GNSs are expected to be synthesised using the library of well-known 1,3-dipolar organic compounds.

Acknowledgements

The authors acknowledge funding from EPSRC Grant No. EP/G007314/1 (M.K.B. and K.S.C.) and EU FP7 4G-PHOTOCAT Grant No. 309636 and EPSRC Grant No. EP/N009533/1 (S.M.).

Notes and references

1. aD. H. Deng, K. S. Novoselov, Q. Fu, N. F. Zheng, Z. Q. Tian and X. H. Bao, *Nature Nanotechnology*, 2016, **11**, 218-230; bC. D. Cress, S. W. Schmucker, A. L. Friedman, P. Dev, J. C. Culbertson, J. W. Lyding and J. T. Robinson, *ACS Nano*, 2016, **10**, 3714-3722; cW. Cai, C. Wang, X. Fang, L. Yang and X. Chen, *Applied Physics Letters*, 2015, **106**, 253105; dD. W. Chang and J. B. Baek, *Chemistry-an Asian Journal*, 2016, **11**, 1125-1137; eL. Feng, L. Yang, Z. Huang, J. Luo, M. Li, D. Wang and Y. Chen, *Scientific Reports*, 2013, **3**, 3306; fY. Liu, L. Yu, C. N. Ong and J. Xie, *Nano Research*, 2016, **9**, 1983-1993; gB. Mendoza-Sanchez and Y. Gogotsi, *Advanced Materials*, 2016, **28**, 6104-6135; hM. Sevilla and A. B. Fuertes, *ACS Nano*, 2014, **8**, 5069-5078; iL. Van Nang, N. Van Duy, N. D. Hoa and N. Van Hieu, *Journal of Electronic Materials*, 2016, **45**, 839-845; jZ. Xing, Z. Ju, Y. Zhao, J. Wan, Y. Zhu, Y. Qiang and Y. Qian, *Scientific Reports*, 2016, **6**, 26146.
2. aL. Qu, Y. Liu, J.-B. Baek and L. Dai, *ACS Nano*, 2010, **4**, 1321-1326; bD. Geng, Y. Chen, Y. Chen, Y. Li, R. Li, X. Sun, S. Ye and S. Knights, *Energy & Environmental Science*, 2011, **4**, 760-764; cL. Lai, J. R. Potts, D. Zhan, L. Wang, C. K. Poh, C. Tang, H. Gong, Z. Shen, J. Lin and R. S. Ruoff, *Energy & Environmental Science*, 2012, **5**, 7936-7942.
3. aH. B. Yang, J. Miao, S.-F. Hung, J. Chen, H. B. Tao, X. Wang, L. Zhang, R. Chen, J. Gao, H. M. Chen, L. Dai and B. Liu, *Science Advances*, 2016, **2**; bD. Guo, R. Shibuya, C. Akiba, S. Saji, T. Kondo and J. Nakamura, *Science*, 2016, **351**, 361-365.
4. aH. Wang, T. Maiyalagan and X. Wang, *ACS Catalysis*, 2012, **2**, 781-794; bP. Bhunia, E. Hwang, Y. Yoon, E. Lee, S. Seo and H. Lee, *Chemistry – A European Journal*, 2012, **18**, 12207-12212.
5. A. Primo, P. Atienzar, E. Sanchez, J. M. Delgado and H. Garcia, *Chemical Communications*, 2012, **48**, 9254-9256.
6. Y. Z. Xue, B. Wu, Q. L. Bao and Y. Q. Liu, *Small*, 2014, **10**, 2975-2991.
7. A. Narita, X. Feng, Y. Hernandez, S. A. Jensen, M. Bonn, H. Yang, I. A. Verzhbitskiy, C. Casiraghi, M. R. Hansen, A. H. R. Koch, G. Fytas, O. Ivasenko, B. Li, K. S. Mali, T. Balandina, S. Mahesh, S. De Feyter and K. Müllen, *Nat Chem*, 2014, **6**, 126-132.
8. J. Cai, P. Ruffieux, R. Jaafar, M. Bieri, T. Braun, S. Blankenburg, M. Muoth, A. P. Seitsonen, M. Saleh, X. Feng, K. Mullen and R. Fasel, *Nature*, 2010, **466**, 470-473.
9. F. Schlutter, T. Nishiuchi, V. Enkelmann and K. Mullen, *Angewandte Chemie-International Edition*, 2014, **53**, 1538-1542.
10. M. K. Bayazit and K. S. Coleman, *Journal of the American Chemical Society*, 2009, **131**, 10670-10676.
11. C. Avendano and A. Briceno, *CrystEngComm*, 2009, **11**, 408-411.
12. C. Najera, J. M. Sansano and M. Yus, *Organic & Biomolecular Chemistry*, 2015, **13**, 8596-8636.
13. aA. Bongers, I. Ranasinghe, P. Lemire, A. Perozzo, J.-F. Vincent-Rocan and A. M. Beauchemin, *Organic Letters*, 2016, **18**, 3778-3781; bN. Dennis, A. R. Katritzky and M. Ramaiah, *Journal of the Chemical Society, Perkin Transactions 1*, 1976, DOI: 10.1039/P19760002281, 2281-2284.
14. M. K. Bayazit and K. S. Coleman, *Chemistry – An Asian Journal*, 2012, **7**, 2925-2930.
15. A. C. Ferrari and D. M. Basko, *Nat Nano*, 2013, **8**, 235-246.
16. Z.-H. Sheng, L. Shao, J.-J. Chen, W.-J. Bao, F.-B. Wang and X.-H. Xia, *ACS Nano*, 2011, **5**, 4350-4358.
17. H. C. Yau, M. K. Bayazit, J. H. G. Steinke and M. S. P. Shaffer, *Chemical Communications*, 2015, **51**, 16621-16624.
18. Y.-F. Lu, S.-T. Lo, J.-C. Lin, W. Zhang, J.-Y. Lu, F.-H. Liu, C.-M. Tseng, Y.-H. Lee, C.-T. Liang and L.-J. Li, *ACS Nano*, 2013, **7**, 6522-6532.
19. C. R. Herron, K. S. Coleman, R. S. Edwards and B. G. Mendis, *Journal of Materials Chemistry*, 2011, **21**, 3378-3383.
20. M. K. Bayazit, L. S. Clarke, K. S. Coleman and N. Clarke, *Journal of the American Chemical Society*, 2010, **132**, 15814-15819.
21. C. Zhang, L. Fu, N. Liu, M. Liu, Y. Wang and Z. Liu, *Advanced Materials*, 2011, **23**, 1020-1024.
22. H. Y. Nan, Z. H. Ni, J. Wang, Z. Zafar, Z. X. Shi and Y. Y. Wang, *Journal of Raman Spectroscopy*, 2013, **44**, 1018-1021.
23. L. S. Panchakarla, K. S. Subrahmanyam, S. K. Saha, A. Govindaraj, H. R. Krishnamurthy, U. V. Waghmare and C. N. R. Rao, *Advanced Materials*, 2009, **21**, 4726-4730.
24. J. R. Pels, F. Kapteijn, J. A. Moulijn, Q. Zhu and K. M. Thomas, *Carbon*, 1995, **33**, 1641-1653.
25. G.-L. Tian, M.-Q. Zhao, D. Yu, X.-Y. Kong, J.-Q. Huang, Q. Zhang and F. Wei, *Small*, 2014, **10**, 2251-2259.
26. M. Li, L. Zhang, Q. Xu, J. Niu and Z. Xia, *Journal of Catalysis*, 2014, **314**, 66-72.
27. M. Gao, W. Sheng, Z. Zhuang, Q. Fang, S. Gu, J. Jiang and Y. Yan, *Journal of the American Chemical Society*, 2014, **136**, 7077-7084.